arXiv:2204.12228v2 [hep-ex] 19 Jul 2023

Measurement of CP asymmetries in $D^+_{(s)} \to \eta\pi^+$ and $D^+_{(s)} \to \eta'\pi^+$ decays

LHCb collaboration[†]

Abstract

Searches for CP violation in the decays $D^+_{(s)} \to \eta\pi^+$ and $D^+_{(s)} \to \eta'\pi^+$ are performed using pp collision data corresponding to 6 fb^{-1} of integrated luminosity collected by the LHCb experiment. The calibration channels $D^+_{(s)} \to \phi\pi^+$ are used to remove production and detection asymmetries. The resulting CP-violating asymmetries are

$$\mathcal{A}^{CP}(D^+ \to \eta\pi^+) = (0.34 \pm 0.66 \pm 0.16 \pm 0.05)\%,$$
$$\mathcal{A}^{CP}(D^+_s \to \eta\pi^+) = (0.32 \pm 0.51 \pm 0.12)\%,$$
$$\mathcal{A}^{CP}(D^+ \to \eta'\pi^+) = (0.49 \pm 0.18 \pm 0.06 \pm 0.05)\%,$$
$$\mathcal{A}^{CP}(D^+_s \to \eta'\pi^+) = (0.01 \pm 0.12 \pm 0.08)\%,$$

where the first uncertainty is statistical, the second is systematic and the third, relevant for the D^+ channels, is due to the uncertainty on $\mathcal{A}^{CP}(D^+ \to \phi\pi^+)$. These measurements, currently the most precise for three of the four channels considered, are consistent with the absence of CP violation. A combination of these results with previous LHCb measurements is presented.

[†]Authors are listed at the end of this paper.

1 Introduction

The observed baryon asymmetry in the Universe requires the violation of the charge-conjugation parity (CP) symmetry [1]. Within the Standard Model (SM), CP violation occurs due to an irreducible complex phase in the Cabibbo-Kobayashi-Maskawa (CKM) matrix, which describes the transitions between quarks [2,3]. However, the size of CP violation in the SM appears to be too small to explain the observed baryon asymmetry, suggesting that there may be additional sources of CP violation beyond the SM [4–6]. Such sources can be associated to new heavy particles, giving further motivation for CP violation searches.

Although CP violation in the b- and s-quark sectors has been established for some time [7–10], its observation in the charm sector was only accomplished in 2019 [11]. The charm sector provides a unique opportunity to study CP violation in decays of up-type quarks. Charge-parity violation in charm decays occurs through the interference of tree- and loop-level diagrams in the Cabibbo-suppressed quark transitions $c \to \bar{d}du$ and $c \to \bar{s}su$. Standard Model calculations of CP violation in the charm sector are difficult due to the presence of low-energy strong-interaction effects; as a consequence, predictions of CP asymmetries vary by orders of magnitude, typically bewteen 10^{-4} and 10^{-2} [12–16]. The study of CP asymmetries in several decays related by flavour symmetry can provide insight to the origin of observed CP violation [17–25]. Of particular interest are two-body decays of D^+ and D_s^+ mesons, such as $D_s^+ \to \eta^{(\prime)}\pi^+$ (Cabibbo-favoured) and $D^+ \to \eta^{(\prime)}\pi^+$ (singly Cabibbo-suppressed).[1] For the singly Cabibbo suppressed decays, predictions for the CP asymmetry from topological-diagram [18] and factorization [20] approaches are, respectively, -0.65×10^{-3} and -0.26×10^{-3} for the $D^+ \to \eta\pi^+$ decay mode. For the $D^+ \to \eta'\pi^+$ channel the corresponding predictions are 0.41×10^{-3} and 1.18×10^{-3}. The CP asymmetries for these channels have been measured by the CLEO [26,27], Belle [28,29] and LHCb [30,31] collaborations. No evidence for CP violation has been observed, within the uncertainties of a few per mil.

This article presents measurements of CP asymmetries for the modes $D_{(s)}^+ \to \eta\pi^+$ and $D_{(s)}^+ \to \eta'\pi^+$ at the LHCb experiment, made using proton-proton (pp) collisions, recorded during the period 2015–2018 at a centre-of-mass energy $\sqrt{s} = 13\,\text{TeV}$, corresponding to an integrated luminosity of 6 fb^{-1}. The η and η' mesons are both reconstructed in the final state $\gamma\pi^+\pi^-$. The two charged particles in the final states allow the reconstruction of the $\eta^{(\prime)}$ decay vertex.

The CP asymmetry is defined as

$$\mathcal{A}^{CP}(D_{(s)}^+ \to f^+) \equiv \frac{\Gamma(D_{(s)}^+ \to f^+) - \Gamma(D_{(s)}^- \to f^-)}{\Gamma(D_{(s)}^+ \to f^+) + \Gamma(D_{(s)}^- \to f^-)}, \tag{1}$$

where f is the considered final state and Γ is the partial decay width. Experimentally, the raw asymmetry $\mathcal{A}^{\text{raw}}$ is measured using the event yields N as

$$\mathcal{A}^{\text{raw}}(D_{(s)}^+ \to f^+) \equiv \frac{N(D_{(s)}^+ \to f^+) - N(D_{(s)}^- \to f^-)}{N(D_{(s)}^+ \to f^+) + N(D_{(s)}^- \to f^-)}. \tag{2}$$

The difference between $\mathcal{A}^{CP}$ and $\mathcal{A}^{\text{raw}}$ arises from asymmetries in the production of positively and negatively charged $D_{(s)}^\pm$ mesons [32,33] and in the detection efficiency of

---

[1]Charge-conjugate decays are implied throughout this article, except when discussing asymmetries.

the corresponding final states. For small asymmetries, $\mathcal{A}^{\text{raw}}$ may be approximated to first order as

$$\mathcal{A}^{\text{raw}}(D_{(s)}^+ \to f^+) \approx \mathcal{A}^{CP}(D_{(s)}^+ \to f^+) + \mathcal{A}^{\text{prod}}(D_{(s)}^+) + \mathcal{A}^{\text{det}}(f^+), \quad (3)$$

where $\mathcal{A}^{\text{prod}} = \frac{\sigma(D_{(s)}^+) - \sigma(D_{(s)}^-)}{\sigma(D_{(s)}^+) + \sigma(D_{(s)}^-)}$ is the production asymmetry and $\mathcal{A}^{\text{det}} = \frac{\epsilon(f^+) - \epsilon(f^-)}{\epsilon(f^+) + \epsilon(f^-)}$ is the detection asymmetry. Here $\sigma(D_{(s)}^\pm)$ is the production cross section for $D_{(s)}^\pm$ mesons and $\epsilon(f^\pm)$ is the efficiency for detecting the final state $f^\pm$. The detection asymmetry can arise due to instrumental effects, such as different interaction cross-sections of positive and negative particles with the detector material, or a small charge-dependence of geometrical effects that are not fully treated in the reconstruction algorithms. For $f^\pm = \eta^{(\prime)}\pi^\pm$, $\mathcal{A}^{\text{det}}$ is due only to the pion, since the decays $\eta^{(\prime)} \to \gamma\pi^+\pi^-$ are charge symmetric.

The production and detection asymmetries are subtracted using the control channels $D_s^+ \to \phi\pi^+$ and $D^+ \to \phi\pi^+$, followed by the decay $\phi \to K^+K^-$. The production and detection asymmetries are the same for the control channels and the signal channels, after accounting for small differences in the kinematic properties, and are therefore eliminated in the difference of the raw asymmetries

$$\mathcal{A}^{\text{raw}}(D^+ \to \eta^{(\prime)}\pi^+) - \mathcal{A}^{\text{raw}}(D^+ \to \phi\pi^+) = \mathcal{A}^{CP}(D^+ \to \eta^{(\prime)}\pi^+) - \mathcal{A}^{CP}(D^+ \to \phi\pi^+), \quad (4)$$

$$\mathcal{A}^{\text{raw}}(D_s^+ \to \eta^{(\prime)}\pi^+) - \mathcal{A}^{\text{raw}}(D_s^+ \to \phi\pi^+) = \mathcal{A}^{CP}(D_s^+ \to \eta^{(\prime)}\pi^+). \quad (5)$$

The Cabibbo-favoured channel $D_s^+ \to \phi\pi^+$ is assumed to have $\mathcal{A}^{CP} = 0$, based on theoretical SM expectations [15]. For the singly Cabibbo-suppressed control channel, the value of $\mathcal{A}^{CP}(D^+ \to \phi\pi^+) = (0.005 \pm 0.051)\%$ [34] is taken as an external input. Its uncertainty is small compared to the sensitivity of this measurement.

2 Detector and simulation

The LHCb detector [35, 36] is a single-arm forward spectrometer covering the pseudorapidity range $2 < \eta < 5$, designed for the study of particles containing b or c quarks. The detector includes a high-precision tracking system consisting of a silicon-strip vertex detector surrounding the pp interaction region, a large-area silicon-strip detector located upstream of a dipole magnet with a bending power of about $4\,\text{Tm}$, and three stations of silicon-strip detectors and straw drift tubes placed downstream of the magnet. The tracking system provides a measurement of the momentum, p, of charged particles with a relative uncertainty that varies from 0.5% at low momentum to 1.0% at $200\,\text{GeV}$.[2] The minimum distance of a track to a primary pp collision vertex (PV), the impact parameter (IP), is measured with a resolution of $(15 + 29/p_{\text{T}})\,\mu\text{m}$, where p_{T} is the component of the momentum transverse to the beam, in GeV. Different types of charged hadrons are distinguished using information from two ring-imaging Cherenkov detectors. Photons, electrons and hadrons are identified by a calorimeter system consisting of scintillating-pad and preshower detectors, an electromagnetic and a hadronic calorimeter. Muons are identified by a system composed of alternating layers of iron and multiwire proportional chambers. The online event selection is performed by a trigger, which consists of a hardware stage, based on information from the calorimeter and muon systems, followed by two software stages, which apply a full event reconstruction. Detector

---

[2]Natural units, with $c = \hbar = 1$, are used throughout.

calibration and alignment is performed after the first software stage and is used in the second stage.

Simulation is required to model the effects of the detector acceptance and the imposed selection requirements, and to study background contributions. In the simulation, pp collisions are generated using PYTHIA [37] with a specific LHCb configuration [38]. Decays of unstable particles are described by EVTGEN [39], in which final-state radiation is generated using PHOTOS [40]. The interaction of the generated particles with the detector, and its response, are implemented using the GEANT4 toolkit [41] as described in Ref. [42].

3 Event selection

The online selection of signal candidates is performed by the trigger. The hardware trigger selects candidates where one or more of the $D_{(s)}^+$ decay products produces a significant energy deposit in the calorimeter. Events where particles that are not used to reconstruct the $D_{(s)}^+$ candidate satisfy the hardware trigger are also accepted. The first software stage requires at least one pion of the $\eta^{(\prime)}$ decay to have high transverse momentum and to be well detached from all primary pp interaction vertices. In the second software stage, each selected event is required to have at least one fully reconstructed $D_{(s)}^+ \to \eta^{(\prime)}\pi^+$ candidate.

Offline, the $\eta^{(\prime)} \to \gamma\pi^+\pi^-$ decays are reconstructed with two oppositely charged well reconstructed tracks and a high-quality photon candidate. A multivariate classifier combining several track-quality criteria is applied to reject fake tracks [36]. Multivariate algorithms based on the shape parameters of the cluster in the electromagnetic calorimeter are used to distinguish the photon from non-electromagnetic deposits associated to hadrons and to reject background in which the two photons are reconstructed as a single cluster [43]. The charged tracks must have transverse momentum $p_{\mathrm{T}} > 500\,\mathrm{MeV}$ and momentum $p > 1000\,\mathrm{MeV}$. Furthermore, they must have particle-identification characteristics compatible with the pion hypothesis. The pion candidates must be well-detached from all primary vertices in the event. Photon candidates must satisfy $p_{\mathrm{T}} > 1000\,\mathrm{MeV}$. For $\eta^\prime$ decays, the invariant mass of the pion pair must be greater than $600\,\mathrm{MeV}$, which selects ρ^0 mesons from the dominant decay process $\eta^\prime \to \rho^0\gamma$, followed by $\rho^0 \to \pi^+\pi^-$. The $\eta^{(\prime)}$ candidates are combined with an additional high-quality track that is consistent with being a pion, denoted the "companion" pion, to form $D_{(s)}^+$ candidates. The companion pion must satisfy $1 < p_{\mathrm{T}} < 20\,\mathrm{GeV}$, have pseudorapidity between 2 and 5, and be significantly detached from all primary vertices. Furthermore, it is required to satisfy fiducial requirements designed to exclude momentum regions for which candidates of one charge are more likely to be deflected out of the detector acceptance, causing large detection asymmetries [11, 34].

The $D_{(s)}^+$ candidates must satisfy $p_{\mathrm{T}} > 2000\,\mathrm{MeV}$ and have proper decay time $\tau > 0.25\,\mathrm{ps}$. Furthermore, the invariant mass of the three pion candidates combined must satisfy $m_{3\pi} < 1825\,\mathrm{MeV}$, which removes background $D_{(s)}^+ \to \pi^+\pi^-\pi^+$ decays. A kinematic fit is performed constraining the three-pion candidates to arise from a common vertex and the $D_{(s)}^+$ candidate to originate at the primary vertex [44]. Selected candidates are required to have a p-value $> 1\%$ for this fit. The invariant mass of the selected candidates is calculated by repeating the kinematic fit while constraining the $\eta^{(\prime)}$ particle to its known mass [45]. The symbols $m(\eta^{(\prime)}\pi^+)$ are used to denote the $D_{(s)}^+$ candidate mass calculated using the $\eta^{(\prime)}$ mass constraint. Multiple candidates are found in 5.5% of

the events. In case of more than one candidate per event, one of the candidates is selected randomly.

The data is divided into eight subsamples, separated by year of data taking, magnet polarity and if the event had multiple primary vertices. The small amount of data from 2015 is combined with the 2016 data. Furthermore, for the years 2015–2017, the dedicated second level software trigger only accepted events with one primary vertex, while for 2018 this requirement was eliminated. The analysis is performed independently on each subsample and a weighted sum is performed to determine the result for the complete dataset.

4 Background sources

The dominant background in all the signal channels is combinatorial, in which random combinations of charged particles and photons result in masses $m(\gamma\pi^+\pi^-)$ and $m(\gamma\pi^+\pi^-\pi^+)$ that are compatible with those of the $\eta^{(\prime)}$ and the $D_{(s)}^+$ mesons, respectively. Included in the combinatorial background is a small contribution from correctly reconstructed $\eta^{(\prime)}$ mesons combined with a random companion pion.

Secondary decays, in which a true $D_{(s)}^+$ meson is the decay product of a b hadron and not produced at the primary vertex, contribute to the signal sample. Such decays can bias the CP asymmetry measurement, because the asymmetry in the production and decay of the b hadron may differ from that of the prompt production of $D_{(s)}^+$ mesons. The secondary background is estimated from simulation to be 11% for the D^+ sample and 13% for the D_s^+ sample. The potential bias introduced by the secondary background is treated as a source of systematic uncertainty (Sec. 7).

Additionally, background arising from the decay channel $D_{(s)}^+ \to \phi\pi^+$, followed by the decay $\phi \to \pi^+\pi^-\pi^0$, (henceforth denoted $D_{(s)}^+ \to \phi_{3\pi}\pi^+$) contributes for the channels with η' in the final state. This can occur when the π^0 meson is misreconstructed as a photon. A component for this background is accounted for in the fit, as discussed in Sec. 5.

Another background contribution comes from the signal decay $D_{(s)}^+ \to \eta\pi^+$, followed by $\eta \to \pi^+\pi^-\pi^0$, with the π^0 meson reconstructed as a photon. This decay is visible in the two-dimensional distribution of $m(\gamma\pi^+\pi^-)$ versus $m(\eta\pi^+)$, as seen in Fig. 1. This background shows only broad peaking behaviour in $m(\eta\pi^+)$ and, in any case, is removed by the selection on $m(\gamma\pi^+\pi^-)$. It should be noted that this decay mode could be used to measure $\mathcal{A}^{CP}(D_{(s)}^+ \to \eta\pi^+)$ with a dedicated analysis.

Other physics background sources from partially or misreconstructed decays, such as $\Lambda_c^+ \to \eta^{(\prime)}p$, $D_{(s)}^+ \to \eta^{(\prime)}\mu^+\nu_\mu$, $D_{(s)}^+ \to \eta^{(\prime)}\pi^+\pi^0$, and $D_{(s)}^+ \to \eta'\pi^+$ (with $\eta' \to \eta\pi^+\pi^-$, $\eta \to \gamma\gamma$), have been studied and found to contribute negligibly in the mass range of interest. The latter two are considered when evaluating the systematic uncertainty associated to the fit model.

5 Determining the raw asymmetry

The distributions of the invariant mass $m(\eta'\pi^\pm)$ of the $D_{(s)}^\pm \to \eta'\pi^\pm$ candidates, separated by charge, are shown in Fig. 2 and the corresponding distributions for the $D_{(s)}^\pm \to \eta\pi^\pm$ candidates are shown in Fig. 3. For each data subsample (described in Sec. 3), the
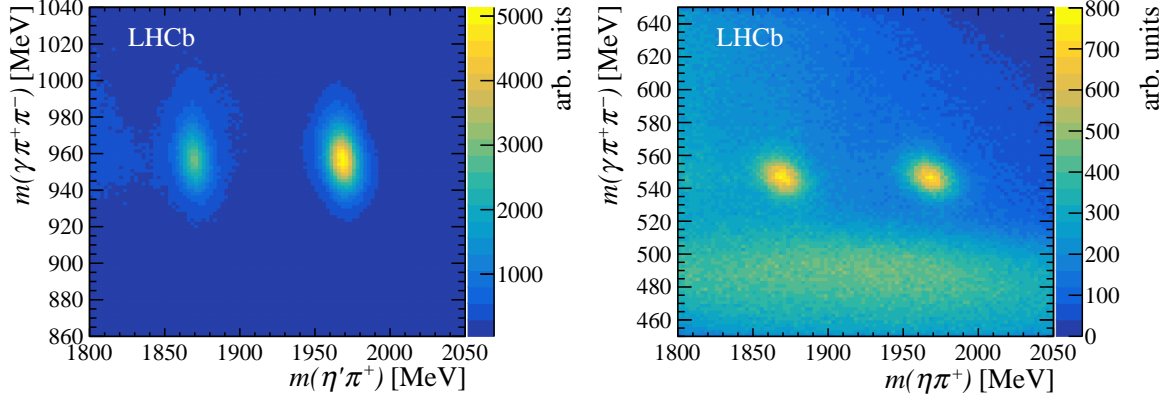
Figure 1: Two-dimensional distributions of $m(\gamma\pi^+\pi^-)$ versus $m(\eta^{(\prime)}\pi^+)$ for (left) the $\eta'\pi^+$ final state and (right) the $\eta\pi^+$ final state. The background candidates at low values of $m(\gamma\pi^+\pi^-)$ for the $\eta\pi^+$ final state arise from $\eta \to \pi^+\pi^-\pi^0$ decays. These distributions correspond to a subset of the signal data sample.
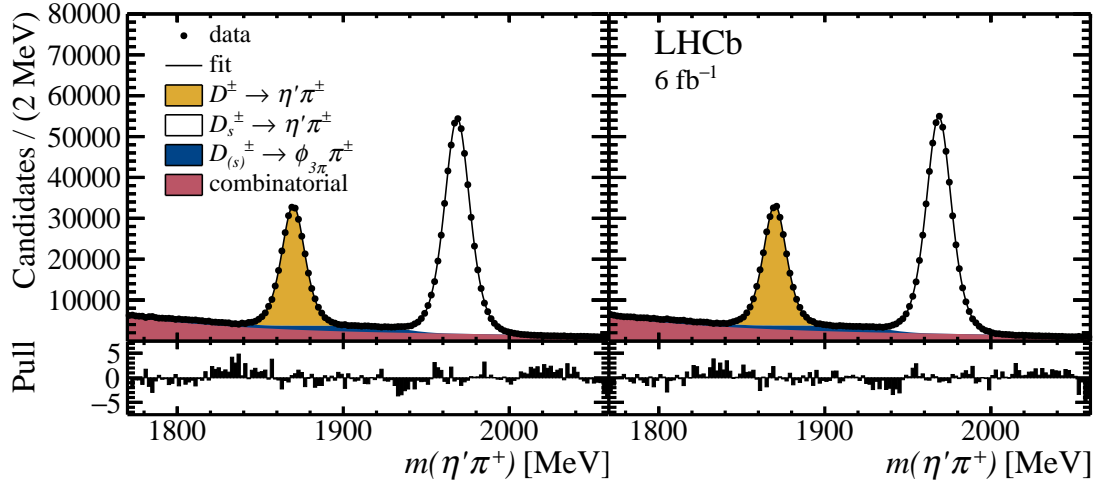

Figure 2: Distribution of the invariant mass $m(\eta'\pi^+)$ of (left) $D_{(s)}^+ \to \eta'\pi^+$ candidates and (right) $D_{(s)}^- \to \eta'\pi^-$ candidates, summed over the eight subsamples. Candidates have $m(\gamma\pi^+\pi^-)$ in the range 936–976 MeV. The results of the fit described in the text are superimposed. The lower panels show the normalised fit residuals (pulls).

raw asymmetry is independently determined using a simultaneous, binned, extended maximum-likelihood fit to the $m(\eta^{(\prime)}\pi^+)$ distributions of positively and negatively charged $D_{(s)}^\pm$ candidates in the mass range 1770–2060 MeV. This fit to the $D_{(s)}^+$ invariant mass is also performed simultaneously in 4 MeV intervals of the unconstrained $m(\gamma\pi^+\pi^-)$ mass, in the mass range 936–976 MeV for the η' channel or 526–570 MeV for the η channel. The distributions of the unconstrained $m(\gamma\pi^+\pi^-)$ mass for $D_{(s)}^+ \to \eta'\pi^+$ and $D_{(s)}^+ \to \eta\pi^+$ candidates are shown in Fig. 4. The total charge-integrated D_s^+ and D^+ yields in each $m(\gamma\pi^+\pi^-)$ bin are also determined in the fit.

The D_s^+ and D^+ mass peaks are each described with a Johnson SU function [46], while the combinatorial background component is modelled by a third-order Chebyshev polynomial. The mean of the Johnson SU function corresponding to the D_s^+ peak is left to
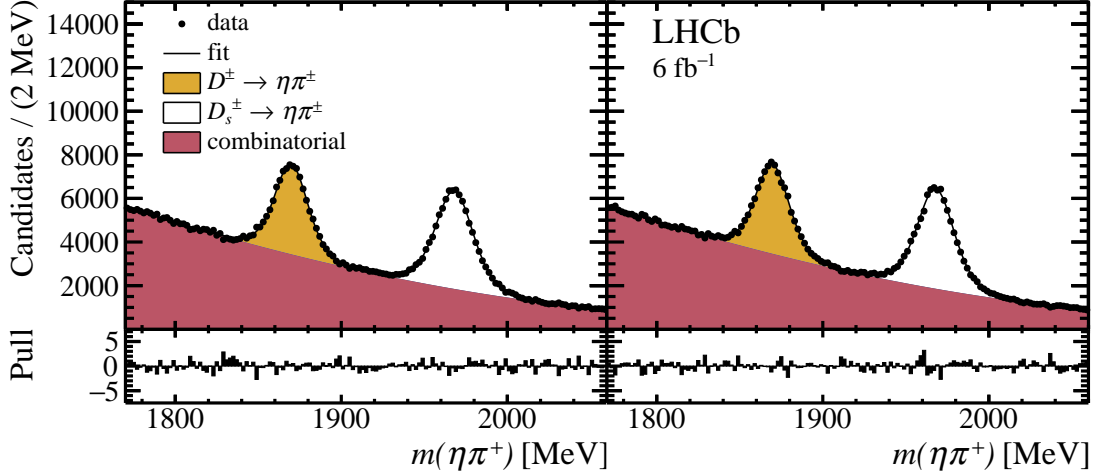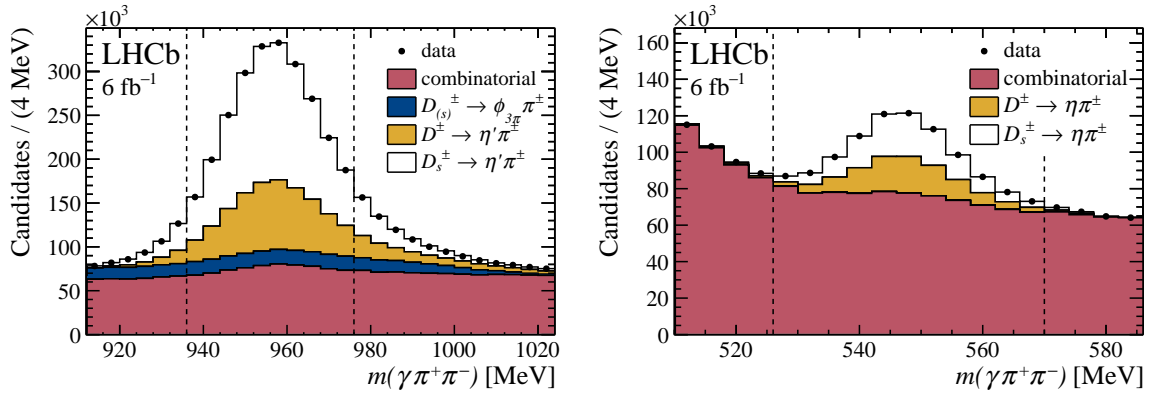
5

Figure 3: Distribution of the invariant mass $m(\eta\pi^+)$ of (left) $D_{(s)}^+ \to \eta\pi^+$ candidates and (right) $D_{(s)}^- \to \eta\pi^-$ candidates, summed over the eight subsamples. Candidates have $m(\gamma\pi^+\pi^-)$ in the range 526–570 MeV. The results of the fit described in the text are superimposed. The lower panels show the normalised fit residuals (pulls).

Figure 4: Distributions of the invariant mass $m(\gamma\pi^+\pi^-)$ for (left) $D_{(s)}^+ \to \eta'\pi^+$ candidates and (right) $D_{(s)}^+ \to \eta\pi^+$ candidates, with the projections of the fit superimposed, summed over the subsamples and the $D_{(s)}^+$ charges. In this figure, the $m(\gamma\pi^+\pi^-)$ mass ranges are enlarged with respect to the baseline fit. The default mass ranges are indicated by the vertical dashed lines.

vary as a function of $m(\gamma\pi^+\pi^-)$. Such variation is expected due to the small correlations between these two quantities. The mean of the Johnson SU function of the D_s^+ peak in the ith $m(\gamma\pi^+\pi^-)$ interval, $\mu_{D_s^+}^i$, is parameterised by

$$\mu_{D_s^+}^i = \mu_{D_s^+}^p + a[M^i - M^p] + b[M^i - M^p]^2, \qquad (6)$$

where M is shorthand for $m(\gamma\pi^+\pi^-)$, and the superscript p refers to the value in the interval corresponding to the peak of the $m(\gamma\pi^+\pi^-)$ distribution. The values of $\mu_{D_s^+}^p$, a and b are determined in the fit. The fit also determines $\Delta m \equiv m(D_s^+) - m(D^+)$, which is allowed to vary linearly as a function of $m(\gamma\pi^+\pi^-)$, thus determining the position of the D^+ peak in each interval of $m(\gamma\pi^+\pi^-)$. Similarly, the widths of both peaks are determined by the fit and allowed to vary quadratically as a function of $m(\gamma\pi^+\pi^-)$. The choice of

6

the allowed variation (linear or quadratic) is made empirically, choosing the simplest functional form that describes the data. These means and widths may be different for positively and negatively charged candidates. The two parameters describing the shape of the tails of the Johnson SU functions are shared among the D_s^+ and D^+ peaks, positively and negatively charged candidates and $m(\gamma\pi^+\pi^-)$ intervals. The background yields and the parameters describing the combinatorial background are determined independently in intervals of $m(\gamma\pi^+\pi^-)$ and for positively and negatively charged candidates.

For the channels $D_{(s)}^+ \to \eta'\pi^+$ a dedicated component to the fit for the background due to $D_{(s)}^+ \to \phi_{3\pi}\pi^+$ decays is included. The shape of this component is obtained from simulated events. The overall yield of this background is free in the fit, while the relative contribution arising from D^+ and D_s^+ decays is fixed to the value estimated from known branching fractions and the relative efficiency determined from simulation.

The results of the fit, summed over the eight subsamples, for the $D_{(s)}^+ \to \eta'\pi^+$ and $D_{(s)}^+ \to \eta\pi^+$ channels are shown in Figs. 2 and 3, respectively. The total charge-integrated signal yields for the $D_s^+ \to \eta'\pi^+$ and $D^+ \to \eta'\pi^+$ channels are $(1\,085.7 \pm 1.2) \times 10^3$ and $(555.4 \pm 0.9) \times 10^3$, respectively. The obtained yields for the $D_s^+ \to \eta\pi^+$ and $D^+ \to \eta\pi^+$ are $(135.8 \pm 0.7) \times 10^3$ and $(110.8 \pm 0.7) \times 10^3$, respectively. The normalised fit residuals (residuals divided by the corresponding uncertainty) for the $D_{(s)}^+ \to \eta'\pi^+$ channel show minor enhancements in correspondence with the endpoint of the of $D_{(s)}^+ \to \phi_{3\pi}\pi^+$ peaking background (whose position is fixed in the fit) and close to the low-mass tail of the $D_{(s)}^+$ signal component. This suggests an imperfect model for this background component, which is treated as a systematic uncertainty (Sec. 7). The normalised fit residuals for the $D_{(s)}^+ \to \eta\pi^+$ channel do not show a similar effect.

The projections of the fit results on $m(\gamma\pi^+\pi^-)$, showing the contribution determined in the fit for each component in each $m(\gamma\pi^+\pi^-)$ interval, are shown in Fig. 4. A small peaking contribution is visible in the combinatorial component, indicating the presence of correctly reconstructed $\eta^{(\prime)}$ candidates paired with random companion pions. For the $D_{(s)}^+ \to \eta\pi^+$ channels, the large shoulder at low values of $m(\gamma\pi^+\pi^-)$, attributed by the fit to the combinatorial component, is due to $D_{(s)}^+ \to \eta\pi^+$ decays, followed by the decay $\eta \to \pi^+\pi^-\pi^0$, as discussed in Sec. 4. This figure was made using wider $m(\gamma\pi^+\pi^-)$ mass ranges than those used for the baseline fit.

6 Control channel analysis

As described in Sec. 1, the control channels $D_{(s)}^+ \to \phi\pi^+$, followed by the decay $\phi \to K^+K^-$, are used to cancel production and detection asymmetries. The triggering and selection of the candidates of the control channels follow closely those of Ref. [34]. In particular, kaon daughters of the ϕ meson are required to satisfy particle-identification criteria compatible with being kaons and the sum of their p_T must be greater than $2\,\mathrm{GeV}$. Their invariant mass $m(K^+K^-)$ must lie in the range 1010–1030 MeV. The pion candidate must have particle-identification information compatible with a pion and $p_T > 1\,\mathrm{GeV}$. As for the signal channels, the pion candidate must satisfy fiducial requirements that remove tracks from areas of the detector with large detector asymmetries. Each $D_{(s)}^+$ candidate must have a large flight distance and a large flight-distance significance. Furthermore, the direction of the momentum of the $D_{(s)}^+$ candidate must be compatible with the direction

defined by its production and decay vertices. The χ^2 per degree of freedom of the vertex fit for the $D_{(s)}^+$ candidate must be small. The $D_{(s)}^+$ candidate transverse momentum must satisfy $p_T > 2700\,\text{MeV}$. These channels have significantly lower background than the signal modes owing to the absence of neutral particles in the final state.

To achieve satisfactory cancellation of production and detector asymmetries, the control sample candidates are weighted such that the distributions of kinematic and trigger variables simultaneously match the distributions observed in the signal sample. Specifically, the distributions of the transverse momentum and pseudorapidity of the companion pion and the $D_{(s)}^+$ candidates, and of the type of trigger decision (whether independent of the final state particles or not) are matched to the signal distributions. The algorithm to determine the weights [47] is trained on distributions from signal and control sample data candidates. The signal distributions are background-subtracted using the *sPlot* technique [48], with $m(\eta^{(\prime)}\pi^+)$ as the discriminating variable; the background in the control sample is negligible.

The control channel data is divided into eight subsamples, as is done for the signal. The invariant mass distribution $m(K^+K^-\pi^\pm)$ for one subsample is shown in Fig. 5. For each subsample, the raw asymmetry is independently determined using a simultaneous binned χ^2 fit to the weighted positive and negative candidates, in the range 1820–1920 MeV for D^+ modes and 1920–2020 MeV for D_s^+ modes. Each control sample channel is fit twice, employing the weighting appropriate for either the $\eta^\prime\pi^+$ or the $\eta\pi^+$ final state. The fit model consists of the sum of a Johnson SU function and a Gaussian function for the $D_{(s)}^+$ peak, and a linear function for the combinatorial background. The parameters describing the tail of the Johnson SU function, the widths of the Johnson SU and Gaussian functions and the relative proportion of the signal described by the Gaussian component are shared among positive and negative candidates. All other fitted parameters are determined separately for positive and negative candidates.

The result of the fit for $\mathcal{A}^{\text{raw}}$ for one control channel subsample, for both the D_s^+ and the D^+ decays, is shown in Fig. 5. The total charge-integrated signal yields for the $D_s^+ \to \phi\pi^+$ and $D^+ \to \phi\pi^+$ channels are $(27\,928 \pm 5) \times 10^3$ and $(16\,276 \pm 4) \times 10^3$, respectively.

7 Systematic uncertainties

Several sources of systematic uncertainty on the CP asymmetry measurements are presented in Table 1. The choice of the fit model to describe the signal mass distributions is a significant source of systematic uncertainty. This is evaluated by fitting, with the baseline model, pseudoexperiments generated according to several alternative models, the parameters of which have been previously determined from the experimental data. In particular, the background model is altered by using a higher-order polynomial function to represent the combinatorial component, including additional background components for partially or misreconstructed decays, or varying their parameterisation, while a sum of two Gaussian functions is used as an alternative parameterisation for the signal. An estimate of the uncertainty caused by possible bias introduced by the fitting procedure is investigated using pseudoexperiments. A significant contribution to the systematic uncertainty also arises from secondary decays, where the $D_{(s)}^+$ is produced in the decay of a b hadron. Such decays have a slightly different value of $\mathcal{A}^{\text{prod}}$, causing a shift in
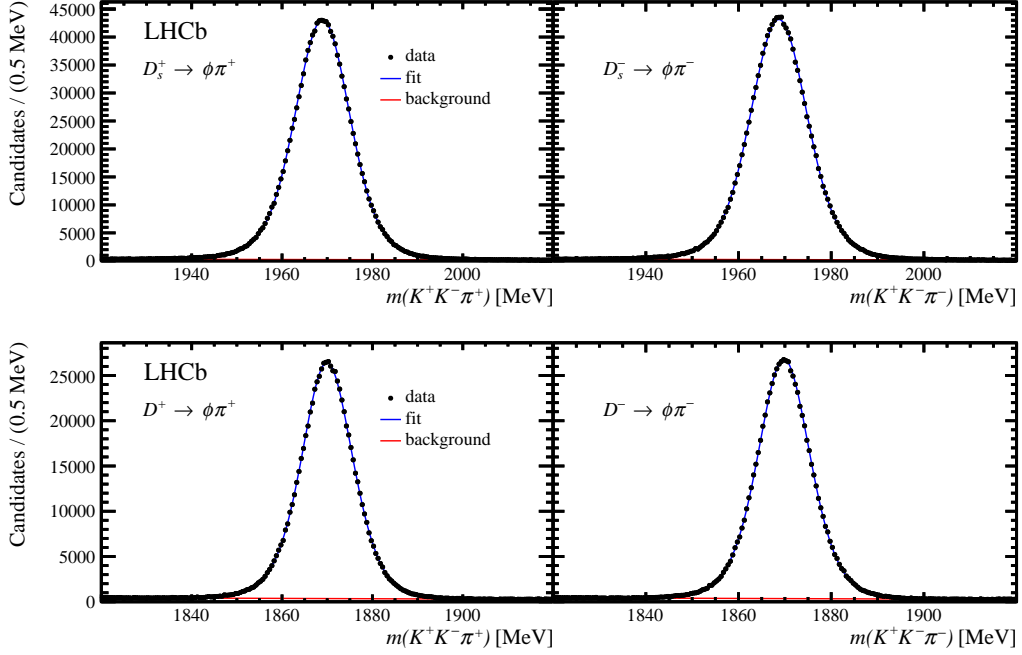
Figure 5: Mass distributions with corresponding fits of (top) $D_s^+ \to \phi\pi^+$ candidates and (bottom) $D^+ \to \phi\pi^+$ candidates. The candidates are weighted to match the signal distributions for the $\eta'\pi^+$ channels. The positively charged candidates are shown on the left and the negatively charged candidates on the right. The blue curves represent the total fit, while the red curves show the very small background component. The data shown are from the 2017, magnet up polarity subsample.

Table 1: Systematic uncertainties associated to values of $\mathcal{A}^{\text{raw}}$ (%).

Source	$D_s^+ \to \eta'\pi^+$	$D^+ \to \eta'\pi^+$	$D_s^+ \to \eta\pi^+$	$D^+ \to \eta\pi^+$
Fit model, signal	0.04	0.04	0.10	0.16
Fit bias	0.01	0.01	0.01	0.02
Secondary decays	0.06	0.03	0.06	0.03
$\mathcal{A}^{\text{KK}}$	0.01	0.02	0.01	0.02
Fit model, control	0.03	0.00	0.03	0.00
Weighting	0.01	0.01	0.02	0.00
Total	0.08	0.06	0.12	0.16

the measured value of $\mathcal{A}^{CP}$. To estimate this contribution, the fraction of secondary background in the signal is derived from simulation, while the production asymmetry of secondary decays is determined on data using a control sample enhanced in such decays.

Sources of systematic uncertainties associated to the analysis of the control channels are also included. The uncertainty due to the fit model of the control channels is determined, as for the signal channels, by considering alternative fit models. Detection asymmetries due to a momentum asymmetry between the kaons in the $\phi \to K^+K^-$ decay have a small associated uncertainty [34]. The systematic uncertainty associated to the weighting procedure is evaluated by repeating the fits to the control channels without performing the weighting, and the resulting shift in $\mathcal{A}^{\text{raw}}$ is taken as the systematic uncertainty.

The systematic uncertainties described here were determined for the full data set, *i.e.* not separately for the different subsamples, and hence are applicable to the final $\mathcal{A}^{CP}$ values given in the next section. The systematic uncertainties for the signal channels and the control channels are added in quadrature.

8 Results

The *CP* asymmetry is obtained by subtracting the value of $\mathcal{A}^{\text{raw}}$ of the control channel from that of the signal channel. For the case of D^+ decays, which are Cabibbo-suppressed, the previously measured value of $\mathcal{A}^{CP}(D^+ \to \phi\pi^+)$ is taken into account, while for Cabibbo-favoured D_s^+ decays, $\mathcal{A}^{CP}(D_s^+ \to \phi\pi^+) = 0$ is assumed, resulting in

$$\mathcal{A}^{CP}(D_s^+ \to \eta^{(\prime)}\pi) = \mathcal{A}^{\text{raw}}(D_s^+ \to \eta^{(\prime)}\pi) - \mathcal{A}^{\text{raw}}(D_s^+ \to \phi\pi^+),$$
$$\mathcal{A}^{CP}(D^+ \to \eta^{(\prime)}\pi) = \mathcal{A}^{\text{raw}}(D^+ \to \eta^{(\prime)}\pi) - \mathcal{A}^{\text{raw}}(D^+ \to \phi\pi^+) + \mathcal{A}^{CP}(D^+ \to \phi\pi^+),$$

where $\mathcal{A}^{CP}(D^+ \to \phi\pi^+) = (0.005 \pm 0.051)\%$ [34].

The results for $\Delta\mathcal{A}^{\text{raw}} = \mathcal{A}^{\text{raw}}(D_{(s)}^+ \to \eta^{(\prime)}\pi^+) - \mathcal{A}^{\text{raw}}(D_{(s)}^+ \to \phi\pi^+)$ for the separate subsamples are shown in Fig. 6. The value of $\mathcal{A}^{CP}$ is determined independently for each of the eight subsamples and a weighted sum is performed to obtain the overall value of $\mathcal{A}^{CP}$, yielding

$$\mathcal{A}^{CP}(D^+ \to \eta\pi^+) = (0.34 \pm 0.66 \pm 0.16 \pm 0.05)\%,$$
$$\mathcal{A}^{CP}(D_s^+ \to \eta\pi^+) = (0.32 \pm 0.51 \pm 0.12)\%,$$
$$\mathcal{A}^{CP}(D^+ \to \eta'\pi^+) = (0.49 \pm 0.18 \pm 0.06 \pm 0.05)\%,$$
$$\mathcal{A}^{CP}(D_s^+ \to \eta'\pi^+) = (0.01 \pm 0.12 \pm 0.08)\%,$$

where the first uncertainty is statistical, the second is systematic and the third, relevant for the D^+ channels, is due to the uncertainty on $\mathcal{A}^{CP}(D^+ \to \phi\pi^+)$. The use of a single control channel for two signal channels, *e.g.*, $D_s^+ \to \phi\pi^+$ for $D^+ \to \eta\pi^+$ and $D^+ \to \eta'\pi^+$, introduces a small correlation between the corresponding $\mathcal{A}^{CP}$ measurements. This correlation is found to be less than 1%.

These results are combined with previous LHCb measurements based on an independent data sample [30] or a different η decay channel [31]. A weighted sum, with weights determined using only the statistical uncertainties, is performed. The systematic uncertainties are uncorrelated between previous and current measurements. The results of the combination are

$$\mathcal{A}^{CP}(D^+ \to \eta\pi^+) = \quad (0.13 \pm 0.50 \pm 0.18)\%,$$
$$\mathcal{A}^{CP}(D_s^+ \to \eta\pi^+) = \quad (0.48 \pm 0.42 \pm 0.17)\%,$$
$$\mathcal{A}^{CP}(D^+ \to \eta'\pi^+) = \quad (0.43 \pm 0.17 \pm 0.10)\%,$$
$$\mathcal{A}^{CP}(D_s^+ \to \eta'\pi^+) = (-0.04 \pm 0.11 \pm 0.09)\%,$$

where the first uncertainty is statistical and the second uncertainty is systematic, which includes the uncertainty on the externally input values of $\mathcal{A}^{CP}$ of the control channels.

In summary, searches for *CP* violation in the decays $D_{(s)}^+ \to \eta\pi^+$ and $D_{(s)}^+ \to \eta'\pi^+$ are performed using *pp* collisions, collected by the LHCb experiment at centre-of-mass
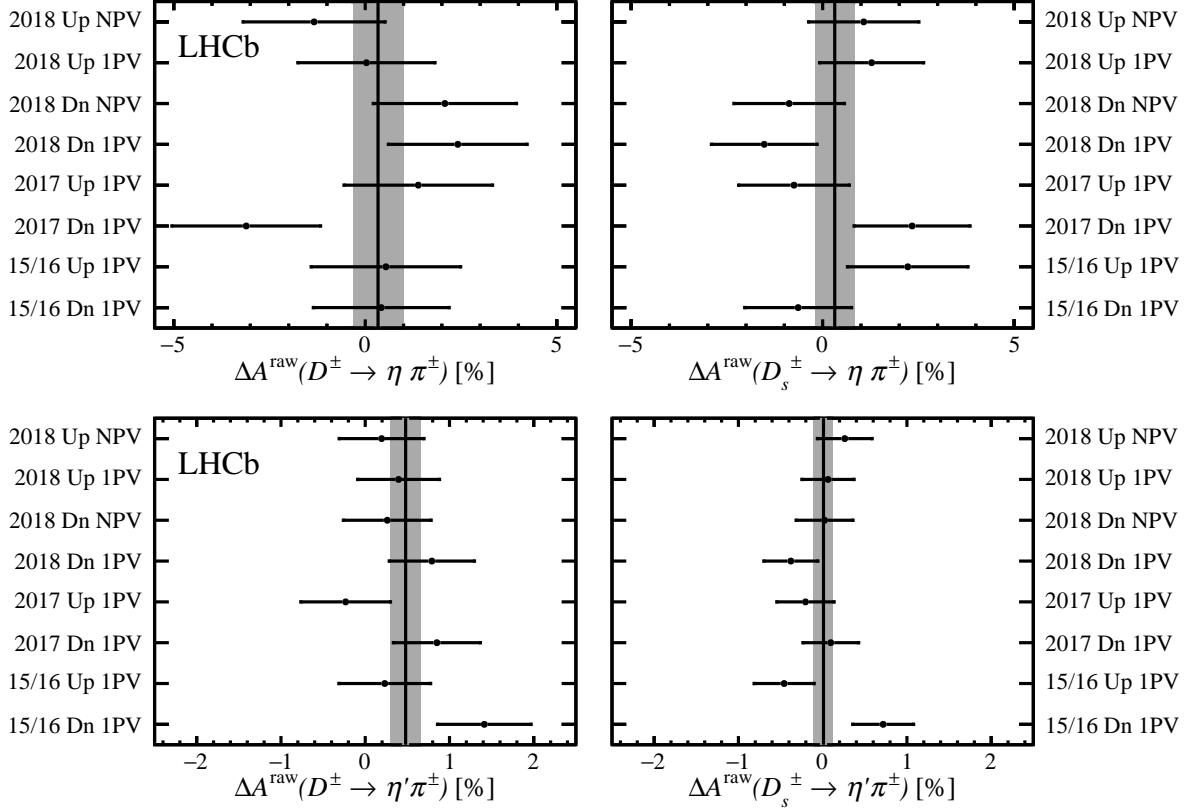
Figure 6: Measured values of $\Delta\mathcal{A}^{\mathrm{raw}}$ for the individual subsamples for (upper left) the $D^+ \to \eta\pi^+$ channel, (upper right) the $D_s^+ \to \eta\pi^+$ channel, (lower left) the $D^+ \to \eta'\pi^+$ channel and (lower right) the $D_s^+ \to \eta'\pi^+$ channel. The subsample labels indicate year of data taking (15/16 = 2015 + 2016), magnet polarity ("Up" or "Dn") and number of PVs ("1PV" for one primary vertex and "NPV" for $N_{\mathrm{PV}} > 1$). The vertical lines and the grey bands indicate the weighted averages and the corresponding statistical uncertainties.

energy $\sqrt{s} = 13$ TeV, corresponding to 6 fb^{-1} of integrated luminosity. The results are consistent with the absence of CP violation in these decay modes and with previous measurements [28–31]. The measurements are the most precise to date for the $D^+ \to \eta\pi^+$, $D^+ \to \eta'\pi^+$ and $D_s^+ \to \eta'\pi^+$ channels.

Acknowledgements

References

[1] A. D. Sakharov, *Violation of CP invariance, C asymmetry, and baryon asymmetry of the universe*, Pisma Zh. Eksp. Teor. Fiz. **5** (1967) 32.

[2] N. Cabibbo, *Unitary symmetry and leptonic decays*, Phys. Rev. Lett. **10** (1963) 531.

[3] M. Kobayashi and T. Maskawa, *CP-violation in the renormalizable theory of weak interaction*, Prog. Theor. Phys. **49** (1973) 652.

[4] A. G. Cohen, D. B. Kaplan, and A. E. Nelson, *Progress in electroweak baryogenesis*, Ann. Rev. Nucl. Part. Sci. **43** (1993) 27, `arXiv:hep-ph/9302210`.

[5] A. Riotto and M. Trodden, *Recent progress in baryogenesis*, Ann. Rev. Nucl. Part. Sci. **49** (1999) 35, `arXiv:hep-ph/9901362`.

[6] W.-S. Hou, *Source of CP violation for the baryon asymmetry of the universe*, Chin. J. Phys. **47** (2009) 134, `arXiv:0803.1234`.

[7] BaBar collaboration, B. Aubert *et al.*, *Observation of direct CP violation in $B^0 \to K^+\pi^-$ decays*, Phys. Rev. Lett. **93** (2004) 131801, `arXiv:hep-ex/0407057`.

[8] Belle collaboration, Y. Chao *et al.*, *Evidence for direct CP violation in $B^0 \to K^+\pi^-$ decays*, Phys. Rev. Lett. **93** (2004) 191802, `arXiv:hep-ex/0408100`.

[9] LHCb collaboration, R. Aaij *et al.*, *First observation of CP violation in the decays of B_s^0 mesons*, Phys. Rev. Lett. **110** (2013) 221601, `arXiv:1304.6173`.

[10] LHCb collaboration, R. Aaij *et al.*, *Observation of CP violation in $B^\pm \to DK^\pm$ decays*, Phys. Lett. **B712** (2012) 203, Erratum ibid. **B713** (2012) 351, `arXiv:1203.3662`.

[11] LHCb collaboration, R. Aaij *et al.*, *Observation of CP violation in charm decays*, Phys. Rev. Lett. **122** (2019) 211803, `arXiv:1903.08726`.

[12] Y. Grossman, A. L. Kagan, and Y. Nir, *New physics and CP violation in singly Cabibbo suppressed D decays*, Phys. Rev. **D75** (2007) 036008, `arXiv:hep-ph/0609178`.

[13] M. Golden and B. Grinstein, *Enhanced CP violations in hadronic charm decays*, Phys. Lett. **B222** (1989) 501.

[14] F. Buccella *et al.*, *Nonleptonic weak decays of charmed mesons*, Phys. Rev. **D51** (1995) 3478, `arXiv:hep-ph/9411286`.

[15] S. Bianco, F. L. Fabbri, D. Benson, and I. Bigi, *A Cicerone for the physics of charm*, Riv. Nuovo Cim. **26** (2003) 1, `arXiv:hep-ex/0309021`.

[16] M. Artuso, B. Meadows, and A. A. Petrov, *Charm Meson Decays*, Ann. Rev. Nucl. Part. Sci. **58** (2008) 249, `arXiv:0802.2934`.

[17] D. Pirtskhalava and P. Uttayarat, *CP Violation and flavor SU(3) breaking in D-meson decays*, Phys. Lett. **B712** (2012) 81, `arXiv:1112.5451`.

[18] H.-Y. Cheng and C.-W. Chiang, *Direct CP violation in two-body hadronic charmed meson decays*, Phys. Rev. **D85** (2012) 034036, `arXiv:1201.0785`, [Erratum: Phys. Rev. **D85**, 079903 (2012)].

[19] T. Feldmann, S. Nandi, and A. Soni, *Repercussions of flavour symmetry breaking on CP violation in D-meson decays*, JHEP **06** (2012) 007, `arXiv:1202.3795`.

[20] H.-n. Li, C.-D. Lu, and F.-S. Yu, *Branching ratios and direct CP asymmetries in $D \to PP$ decays*, Phys. Rev. **D86** (2012) 036012, `arXiv:1203.3120`.

[21] E. Franco, S. Mishima, and L. Silvestrini, *The Standard Model confronts CP violation in $D^0 \to \pi^+\pi^-$ and $D^0 \to K^+K^-$*, JHEP **05** (2012) 140, `arXiv:1203.3131`.

[22] J. Brod, Y. Grossman, A. L. Kagan, and J. Zupan, *A consistent picture for large penguins in $D \to \pi^+\pi^-, K^+K^-$*, JHEP **10** (2012) 161, `arXiv:1203.6659`.

[23] D. Atwood and A. Soni, *Searching for the origin of CP violation in Cabibbo suppressed D-meson decays*, PTEP **2013** (2013) 093B05, `arXiv:1211.1026`.

[24] G. Hiller, M. Jung, and S. Schacht, *SU(3)-flavor anatomy of nonleptonic charm decays*, Phys. Rev. **D87** (2013) 014024, `arXiv:1211.3734`.

[25] S. Müller, U. Nierste, and S. Schacht, *Sum rules of charm CP asymmetries beyond the $SU(3)_F$ limit*, Phys. Rev. Lett. **115** (2015) 251802, `arXiv:1506.04121`.

[26] CLEO collaboration, H. Mendez *et al.*, *Measurements of D meson decays to two pseudoscalar mesons*, Phys. Rev. **D81** (2010) 052013, `arXiv:0906.3198`.

[27] CLEO collaboration, P. U. E. Onyisi *et al.*, *Improved measurement of absolute hadronic branching fractions of the D_s^+ meson*, Phys. Rev. **D88** (2013) 032009, `arXiv:1306.5363`.

[28] Belle collaboration, E. Won *et al.*, *Observation of $D^+ \to K^+\eta^{(\prime)}$ and search for CP violation in $D^+ \to \pi^+\eta^{(\prime)}$ decays*, Phys. Rev. Lett. **107** (2011) 221801, `arXiv:1107.0553`.

[29] Belle collaboration, Y. Guan *et al.*, *Measurement of branching fractions and CP asymmetries for $D_s^+ \to K^+(\eta, \pi^0)$ and $D_s^+ \to \pi^+(\eta, \pi^0)$ decays at Belle*, Phys. Rev. **D103** (2021) 112005, `arXiv:2103.09969`.

[30] LHCb collaboration, R. Aaij *et al.*, *Measurement of CP asymmetries in $D^\pm \to \eta'\pi^\pm$ and $D_s^\pm \to \eta'\pi^\pm$ decays*, Phys. Lett. **B771** (2017) 21, `arXiv:1701.01871`.

[31] LHCb collaboration, R. Aaij *et al.*, *Search for CP violation in* $D_{(s)}^+ \to h^+\pi^0$ *and* $D_{(s)}^+ \to h^+\eta$ *decays*, JHEP **06** (2021) 019, arXiv:2103.11058.

[32] LHCb collaboration, R. Aaij *et al.*, *Measurement of* $D_s^\pm$ *production asymmetry in pp collisions at* $\sqrt{s} = 7$ *and 8 TeV*, JHEP **08** (2018) 008, arXiv:1805.09869.

[33] LHCb collaboration, R. Aaij *et al.*, *Measurement of the* $D^\pm$ *production asymmetry in 7 TeV pp collisions*, Phys. Lett. **B718** (2013) 902, arXiv:1210.4112.

[34] LHCb collaboration, R. Aaij *et al.*, *Search for CP violation in* $D_s^+ \to K_S^0\pi^+$, $D^+ \to K_S^0 K^+$ *and* $D^+ \to \phi\pi^+$ *decays*, Phys. Rev. Lett. **122** (2019) 191803, arXiv:1903.01150.

[35] LHCb collaboration, A. A. Alves Jr. *et al.*, *The LHCb detector at the LHC*, JINST **3** (2008) S08005.

[36] LHCb collaboration, R. Aaij *et al.*, *LHCb detector performance*, Int. J. Mod. Phys. **A30** (2015) 1530022, arXiv:1412.6352.

[37] T. Sjöstrand, S. Mrenna, and P. Skands, *A brief introduction to PYTHIA 8.1*, Comput. Phys. Commun. **178** (2008) 852, arXiv:0710.3820; T. Sjöstrand, S. Mrenna, and P. Skands, *PYTHIA 6.4 physics and manual*, JHEP **05** (2006) 026, arXiv:hep-ph/0603175.

[38] I. Belyaev *et al.*, *Handling of the generation of primary events in Gauss, the LHCb simulation framework*, J. Phys. Conf. Ser. **331** (2011) 032047.

[39] D. J. Lange, *The EvtGen particle decay simulation package*, Nucl. Instrum. Meth. **A462** (2001) 152.

[40] N. Davidson, T. Przedzinski, and Z. Was, *PHOTOS interface in C++: Technical and physics documentation*, Comp. Phys. Comm. **199** (2016) 86, arXiv:1011.0937.

[41] Geant4 collaboration, J. Allison *et al.*, *Geant4 developments and applications*, IEEE Trans. Nucl. Sci. **53** (2006) 270; Geant4 collaboration, S. Agostinelli *et al.*, *Geant4: A simulation toolkit*, Nucl. Instrum. Meth. **A506** (2003) 250.

[42] M. Clemencic *et al.*, *The LHCb simulation application, Gauss: Design, evolution and experience*, J. Phys. Conf. Ser. **331** (2011) 032023.

[43] C. Abellan Beteta *et al.*, *Calibration and performance of the LHCb calorimeters in Run 1 and 2 at the LHC*, arXiv:2008.11556, submitted to JINST.

[44] W. D. Hulsbergen, *Decay chain fitting with a Kalman filter*, Nucl. Instrum. Meth. **A552** (2005) 566, arXiv:physics/0503191.

[45] Particle Data Group, P. A. Zyla *et al.*, *Review of particle physics*, Prog. Theor. Exp. Phys. **2020** (2020) 083C01.

[46] N. L. Johnson, *Systems of frequency curves generated by methods of translation*, Biometrika **36** (1949) 149.

[47] A. Rogozhnikov, *Reweighting with boosted decision trees*, J. Phys. Conf. Ser. **762** (2016) 012036, arXiv:1608.05806.

[48] M. Pivk and F. R. Le Diberder, *sPlot: A statistical tool to unfold data distributions*, Nucl. Instrum. Meth. **A555** (2005) 356, arXiv:physics/0402083.

LHCb collaboration

R. Aaij[32], A.S.W. Abdelmotteleb[50], C. Abellan Beteta[44], F. Abudinén[50],
T. Ackernley[54], B. Adeva[40], M. Adinolfi[48], H. Afsharnia[9], C. Agapopoulou[13],
C.A. Aidala[77], S. Aiola[25], Z. Ajaltouni[9], S. Akar[59], K. Akiba[32], J. Albrecht[15],
F. Alessio[42], M. Alexander[53], A. Alfonso Albero[39], Z. Aliouche[56],
P. Alvarez Cartelle[49], S. Amato[2], J.L. Amey[48], Y. Amhis[11], L. An[42],
L. Anderlini[22], M. Andersson[44], A. Andreianov[38], M. Andreotti[21], D. Ao[6],
F. Archilli[17], A. Artamonov[38], M. Artuso[62], K. Arzymatov[38], E. Aslanides[10],
M. Atzeni[44], B. Audurier[12], S. Bachmann[17], M. Bachmayer[43], J.J. Back[50],
A. Bailly-reyre[13], P. Baladron Rodriguez[40], V. Balagura[12], W. Baldini[21],
J. Baptista de Souza Leite[1], M. Barbetti[22,j], R.J. Barlow[56], S. Barsuk[11],
W. Barter[55], M. Bartolini[49], F. Baryshnikov[38], J.M. Basels[14], G. Bassi[29,q],
B. Batsukh[4], A. Battig[15], A. Bay[43], A. Beck[50], M. Becker[15], F. Bedeschi[29],
I.B. Bediaga[1], A. Beiter[62], V. Belavin[38], S. Belin[40], V. Bellee[44], K. Belous[38],
I. Belov[38], I. Belyaev[38], G. Bencivenni[23], E. Ben-Haim[13], A. Berezhnoy[38],
R. Bernet[44], D. Berninghoff[17], H.C. Bernstein[62], C. Bertella[56], A. Bertolin[28],
C. Betancourt[44], F. Betti[42], Ia. Bezshyiko[44], S. Bhasin[48], J. Bhom[35], L. Bian[67],
M.S. Bieker[15], N.V. Biesuz[21], S. Bifani[47], P. Billoir[13], A. Biolchini[32], M. Birch[55],
F.C.R. Bishop[49], A. Bitadze[56], A. Bizzeti, M. Bjørn[57], M.P. Blago[49], T. Blake[50],
F. Blanc[43], S. Blusk[62], D. Bobulska[53], J.A. Boelhauve[15], O. Boente Garcia[40],
T. Boettcher[59], A. Boldyrev[38], N. Bondar[38,42], S. Borghi[56], M. Borisyak[38],
M. Borsato[17], J.T. Borsuk[35], S.A. Bouchiba[43], T.J.V. Bowcock[54,42], A. Boyer[42],
C. Bozzi[21], M.J. Bradley[55], S. Braun[60], A. Brea Rodriguez[40], J. Brodzicka[35],
A. Brossa Gonzalo[50], D. Brundu[27], A. Buonaura[44], L. Buonincontri[28],
A.T. Burke[56], C. Burr[42], A. Bursche[66], A. Butkevich[38], J.S. Butter[32],
J. Buytaert[42], W. Byczynski[42], S. Cadeddu[27], H. Cai[67], R. Calabrese[21,i],
L. Calefice[15,13], S. Cali[23], R. Calladine[47], M. Calvi[26,m], M. Calvo Gomez[75],
P. Camargo Magalhaes[48], P. Campana[23], A.F. Campoverde Quezada[6], S. Capelli[26,m],
L. Capriotti[20,g], A. Carbone[20,g], G. Carboni[31], R. Cardinale[24,k], A. Cardini[27],
I. Carli[4], P. Carniti[26,m], L. Carus[14], A. Casais Vidal[40], R. Caspary[17], G. Casse[54],
M. Cattaneo[42], G. Cavallero[42], V. Cavallini[21,i], S. Celani[43], J. Cerasoli[10],
D. Cervenkov[57], A.J. Chadwick[54], M.G. Chapman[48], M. Charles[13], Ph. Charpentier[42],
C.A. Chavez Barajas[54], M. Chefdeville[8], C. Chen[3], S. Chen[4], A. Chernov[35],
V. Chobanova[40], S. Cholak[43], M. Chrzaszcz[35], A. Chubykin[38], V. Chulikov[38],
P. Ciambrone[23], M.F. Cicala[50], X. Cid Vidal[40], G. Ciezarek[42], P.E.L. Clarke[52],
M. Clemencic[42], H.V. Cliff[49], J. Closier[42], J.L. Cobbledick[56], V. Coco[42],
J.A.B. Coelho[11], J. Cogan[10], E. Cogneras[9], L. Cojocariu[37], P. Collins[42],
T. Colombo[42], L. Congedo[19,f], A. Contu[27], N. Cooke[47], G. Coombs[53],
I. Corredoira[40], G. Corti[42], C.M. Costa Sobral[50], B. Couturier[42], D.C. Craik[58],
J. Crkovská[61], M. Cruz Torres[1,e], R. Currie[52], C.L. Da Silva[61], S. Dadabaev[38],
L. Dai[65], E. Dall'Occo[15], J. Dalseno[40], C. D'Ambrosio[42], A. Danilina[38],
P. d'Argent[42], J.E. Davies[56], A. Davis[56], O. De Aguiar Francisco[56], J. de Boer[42],
K. De Bruyn[73], S. De Capua[56], M. De Cian[43], U. De Freitas Carneiro Da Graca[1],
E. De Lucia[23], J.M. De Miranda[1], L. De Paula[2], M. De Serio[19,f], D. De Simone[44],
P. De Simone[23], F. De Vellis[15], J.A. de Vries[74], C.T. Dean[61], F. Debernardis[19,f],
D. Decamp[8], V. Dedu[10], L. Del Buono[13], B. Delaney[49], H.-P. Dembinski[15],
V. Denysenko[44], O. Deschamps[9], F. Dettori[27,h], B. Dey[71], A. Di Cicco[23],
P. Di Nezza[23], S. Didenko[38], L. Dieste Maronas[40], H. Dijkstra[42], S. Ding[62],
V. Dobishuk[46], C. Dong[3], A.M. Donohoe[18], F. Dordei[27], A.C. dos Reis[1],

L. Douglas[53], A.G. Downes[8], M.W. Dudek[35], L. Dufour[42], V. Duk[72], P. Durante[42],
J.M. Durham[61], D. Dutta[56], A. Dziurda[35], A. Dzyuba[38], S. Easo[51], U. Egede[63],
V. Egorychev[38], S. Eidelman[38,†], S. Eisenhardt[52], S. Ek-In[43], L. Eklund[76], S. Ely[62],
A. Ene[37], E. Epple[61], S. Escher[14], J. Eschle[44], S. Esen[44], T. Evans[56],
L.N. Falcao[1], Y. Fan[6], B. Fang[67], S. Farry[54], D. Fazzini[26,m], M. Feo[42],
A. Fernandez Prieto[40], A.D. Fernez[60], F. Ferrari[20], L. Ferreira Lopes[43],
F. Ferreira Rodrigues[2], S. Ferreres Sole[32], M. Ferrillo[44], M. Ferro-Luzzi[42],
S. Filippov[38], R.A. Fini[19], M. Fiorini[21,i], M. Firlej[34], K.M. Fischer[57],
D.S. Fitzgerald[77], C. Fitzpatrick[56], T. Fiutowski[34], F. Fleuret[12], M. Fontana[13],
F. Fontanelli[24,k], R. Forty[42], D. Foulds-Holt[49], V. Franco Lima[54],
M. Franco Sevilla[60], M. Frank[42], E. Franzoso[21,i], G. Frau[17], C. Frei[42],
D.A. Friday[53], J. Fu[6], Q. Fuehring[15], E. Gabriel[32], G. Galati[19,f],
A. Gallas Torreira[40], D. Galli[20,g], S. Gambetta[52,42], Y. Gan[3], M. Gandelman[2],
P. Gandini[25], Y. Gao[5], M. Garau[27], L.M. Garcia Martin[50], P. Garcia Moreno[39],
J. García Pardiñas[26,m], B. Garcia Plana[40], F.A. Garcia Rosales[12], L. Garrido[39],
C. Gaspar[42], R.E. Geertsema[32], D. Gerick[17], L.L. Gerken[15], E. Gersabeck[56],
M. Gersabeck[56], T. Gershon[50], D. Gerstel[10], L. Giambastiani[28], V. Gibson[49],
H.K. Giemza[36], A.L. Gilman[57], M. Giovannetti[23,t], A. Gioventù[40],
P. Gironella Gironell[39], C. Giugliano[21,i], K. Gizdov[52], E.L. Gkougkousis[42],
V.V. Gligorov[13,42], C. Göbel[64], E. Golobardes[75], D. Golubkov[38], A. Golutvin[55,38],
A. Gomes[1,a], S. Gomez Fernandez[39], F. Goncalves Abrantes[57], M. Goncerz[35],
G. Gong[3], I.V. Gorelov[38], C. Gotti[26], J.P. Grabowski[17], T. Grammatico[13],
L.A. Granado Cardoso[42], E. Graugés[39], E. Graverini[43], G. Graziani, A. T. Grecu[37],
L.M. Greeven[32], N.A. Grieser[4], L. Grillo[56], S. Gromov[38], B.R. Gruberg Cazon[57], C.
Gu[3], M. Guarise[21,i], M. Guittiere[11], P. A. Günther[17], E. Gushchin[38], A. Guth[14],
Y. Guz[38], T. Gys[42], T. Hadavizadeh[63], G. Haefeli[43], C. Haen[42], J. Haimberger[42],
S.C. Haines[49], T. Halewood-leagas[54], M.M. Halvorsen[42], P.M. Hamilton[60],
J. Hammerich[54], Q. Han[7], X. Han[17], E.B. Hansen[56], S. Hansmann-Menzemer[17],
N. Harnew[57], T. Harrison[54], C. Hasse[42], M. Hatch[42], J. He[6,c], M. Hecker[55],
K. Heijhoff[32], K. Heinicke[15], R.D.L. Henderson[63,50], A.M. Hennequin[42],
K. Hennessy[54], L. Henry[42], J. Heuel[14], A. Hicheur[2], D. Hill[43], M. Hilton[56],
S.E. Hollitt[15], R. Hou[7], Y. Hou[8], J. Hu[17], J. Hu[66], W. Hu[7], X. Hu[3],
W. Huang[6], X. Huang[67], W. Hulsbergen[32], R.J. Hunter[50], M. Hushchyn[38],
D. Hutchcroft[54], D. Hynds[32], P. Ibis[15], M. Idzik[34], D. Ilin[38], P. Ilten[59],
A. Inglessi[38], A. Ishteev[38], K. Ivshin[38], R. Jacobsson[42], H. Jage[14], S. Jakobsen[42],
E. Jans[32], B.K. Jashal[41], A. Jawahery[60], V. Jevtic[15], X. Jiang[4,6], M. John[57],
D. Johnson[58], C.R. Jones[49], T.P. Jones[50], B. Jost[42], N. Jurik[42], S. Kandybei[45],
Y. Kang[3], M. Karacson[42], D. Karpenkov[38], M. Karpov[38], J.W. Kautz[59],
F. Keizer[42], D.M. Keller[62], M. Kenzie[50], T. Ketel[33], B. Khanji[15], A. Kharisova[38],
S. Kholodenko[38], T. Kirn[14], V.S. Kirsebom[43], O. Kitouni[58], S. Klaver[33],
N. Kleijne[29,q], K. Klimaszewski[36], M.R. Kmiec[36], S. Koliiev[46], A. Kondybayeva[38],
A. Konoplyannikov[38], P. Kopciewicz[34], R. Kopecna[17], P. Koppenburg[32], M. Korolev[38],
I. Kostiuk[32,46], O. Kot[46], S. Kotriakhova, A. Kozachuk[38], P. Kravchenko[38],
L. Kravchuk[38], R.D. Krawczyk[42], M. Kreps[50], S. Kretzschmar[14], P. Krokovny[38],
W. Krupa[34], W. Krzemien[36], J. Kubat[17], W. Kucewicz[35,34], M. Kucharczyk[35],
V. Kudryavtsev[38], H.S. Kuindersma[32], G.J. Kunde[61], T. Kvaratskheliya[38], D. Lacarrere[42],
G. Lafferty[56], A. Lai[27], A. Lampis[27], D. Lancierini[44], J.J. Lane[56], R. Lane[48],
G. Lanfranchi[23], C. Langenbruch[14], J. Langer[15], O. Lantwin[38], T. Latham[50],
F. Lazzari[29,u], M. Lazzaroni[25], R. Le Gac[10], S.H. Lee[77], R. Lefèvre[9], A. Leflat[38],
S. Legotin[38], O. Leroy[10], T. Lesiak[35], B. Leverington[17], H. Li[66], P. Li[17],

S. Li[7], Y. Li[4], Z. Li[62], X. Liang[62], T. Lin[55], R. Lindner[42], V. Lisovskyi[15],
R. Litvinov[27], G. Liu[66], H. Liu[6], Q. Liu[6], S. Liu[4,6], A. Lobo Salvia[39],
A. Loi[27], R. Lollini[72], J. Lomba Castro[40], I. Longstaff[53], J.H. Lopes[2],
S. López Soliño[40], G.H. Lovell[49], Y. Lu[4,b], C. Lucarelli[22,j], D. Lucchesi[28,o],
S. Luchuk[38], M. Lucio Martinez[32], V. Lukashenko[32,46], Y. Luo[3], A. Lupato[56],
E. Luppi[21,i], O. Lupton[50], A. Lusiani[29,q], X.-R. Lyu[6], L. Ma[4], R. Ma[6],
S. Maccolini[20], F. Machefert[11], F. Maciuc[37], V. Macko[43], P. Mackowiak[15],
S. Maddrell-Mander[48], L.R. Madhan Mohan[48], A. Maevskiy[38], D. Maisuzenko[38],
M.W. Majewski[34], J.J. Malczewski[35], S. Malde[57], B. Malecki[35], A. Malinin[38],
T. Maltsev[38], H. Malygina[17], G. Manca[27,h], G. Mancinelli[10], D. Manuzzi[20],
C.A. Manzari[44], D. Marangotto[25,l], J.M. Maratas[9,w], J.F. Marchand[8],
U. Marconi[20], S. Mariani[22,j], C. Marin Benito[42], M. Marinangeli[43], J. Marks[17],
A.M. Marshall[48], P.J. Marshall[54], G. Martelli[72,p], G. Martellotti[30],
L. Martinazzoli[42,m], M. Martinelli[26,m], D. Martinez Santos[40], F. Martinez Vidal[41],
A. Massafferri[1], M. Materok[14], R. Matev[42], A. Mathad[44], V. Matiunin[38],
C. Matteuzzi[26], K.R. Mattioli[77], A. Mauri[32], E. Maurice[12], J. Mauricio[39],
M. Mazurek[42], M. McCann[55], L. Mcconnell[18], T.H. McGrath[56], N.T. McHugh[53],
A. McNab[56], R. McNulty[18], J.V. Mead[54], B. Meadows[59], G. Meier[15],
D. Melnychuk[36], S. Meloni[26,m], M. Merk[32,74], A. Merli[25,l], L. Meyer Garcia[2],
M. Mikhasenko[69,d], D.A. Milanes[68], E. Millard[50], M. Milovanovic[42], M.-N. Minard[8,†],
A. Minotti[26,m], S.E. Mitchell[52], B. Mitreska[56], D.S. Mitzel[15], A. Mödden [15],
R.A. Mohammed[57], R.D. Moise[55], S. Mokhnenko[38], T. Mombächer[40],
I.A. Monroy[68], S. Monteil[9], M. Morandin[28], G. Morello[23], M.J. Morello[29,q],
J. Moron[34], A.B. Morris[69], A.G. Morris[50], R. Mountain[62], H. Mu[3], F. Muheim[52],
M. Mulder[73], K. Müller[44], C.H. Murphy[57], D. Murray[56], R. Murta[55],
P. Muzzetto[27], P. Naik[48], T. Nakada[43], R. Nandakumar[51], T. Nanut[42],
I. Nasteva[2], M. Needham[52], N. Neri[25,l], S. Neubert[69], N. Neufeld[42], P. Neustroev[38],
R. Newcombe[55], E.M. Niel[43], S. Nieswand[14], N. Nikitin[38], N.S. Nolte[58], C. Normand[8],
C. Nunez[77], A. Oblakowska-Mucha[34], V. Obraztsov[38], T. Oeser[14],
D.P. O'Hanlon[48], S. Okamura[21,i], R. Oldeman[27,h], F. Oliva[52], M.E. Olivares[62],
C.J.G. Onderwater[73], R.H. O'Neil[52], J.M. Otalora Goicochea[2], T. Ovsiannikova[38],
P. Owen[44], A. Oyanguren[41], O. Ozcelik[52], K.O. Padeken[69], B. Pagare[50],
P.R. Pais[42], T. Pajero[57], A. Palano[19], M. Palutan[23], Y. Pan[56], G. Panshin[38],
A. Papanestis[51], M. Pappagallo[19,f], L.L. Pappalardo[21,i], C. Pappenheimer[59],
W. Parker[60], C. Parkes[56], B. Passalacqua[21,i], G. Passaleva[22], A. Pastore[19],
M. Patel[55], C. Patrignani[20,g], C.J. Pawley[74], A. Pearce[42], A. Pellegrino[32],
M. Pepe Altarelli[42], S. Perazzini[20], D. Pereima[38], A. Pereiro Castro[40], P. Perret[9],
M. Petric[53], K. Petridis[48], A. Petrolini[24,k], A. Petrov[38], S. Petrucci[52], M. Petruzzo[25],
H. Pham[62], A. Philippov[38], R. Piandani[6], L. Pica[29,q], M. Piccini[72], B. Pietrzyk[8],
G. Pietrzyk[11], M. Pili[57], D. Pinci[30], F. Pisani[42], M. Pizzichemi[26,m,42],
V. Placinta[37], J. Plews[47], M. Plo Casasus[40], F. Polci[13,42], M. Poli Lener[23],
M. Poliakova[62], A. Poluektov[10], N. Polukhina[38], I. Polyakov[62], E. Polycarpo[2],
S. Ponce[42], D. Popov[6,42], S. Popov[38], S. Poslavskii[38], K. Prasanth[35],
L. Promberger[42], C. Prouve[40], V. Pugatch[46], V. Puill[11], G. Punzi[29,r], H.R. Qi[3],
W. Qian[6], N. Qin[3], R. Quagliani[43], N.V. Raab[18], R.I. Rabadan Trejo[6],
B. Rachwal[34], J.H. Rademacker[48], R. Rajagopalan[62], M. Rama[29],
M. Ramos Pernas[50], M.S. Rangel[2], F. Ratnikov[38], G. Raven[33,42], M. Reboud[8],
F. Redi[42], F. Reiss[56], C. Remon Alepuz[41], Z. Ren[3], V. Renaudin[57], P.K. Resmi[10],
R. Ribatti[29,q], A.M. Ricci[27], S. Ricciardi[51], K. Rinnert[54], P. Robbe[11],
G. Robertson[52], A.B. Rodrigues[43], E. Rodrigues[54], J.A. Rodriguez Lopez[68],

E. Rodriguez Rodriguez[40], A. Rollings[57], P. Roloff[42], V. Romanovskiy[38],
M. Romero Lamas[40], A. Romero Vidal[40], J.D. Roth[77,†], M. Rotondo[23],
M.S. Rudolph[62], T. Ruf[42], R.A. Ruiz Fernandez[40], J. Ruiz Vidal[41], A. Ryzhikov[38],
J. Ryzka[34], J.J. Saborido Silva[40], N. Sagidova[38], N. Sahoo[47], B. Saitta[27,h],
M. Salomoni[42], C. Sanchez Gras[32], R. Santacesaria[30], C. Santamarina Rios[40],
M. Santimaria[23], E. Santovetti[31,t], D. Saranin[38], G. Sarpis[14], M. Sarpis[69],
A. Sarti[30], C. Satriano[30,s], A. Satta[31], M. Saur[15], D. Savrina[38], H. Sazak[9],
L.G. Scantlebury Smead[57], A. Scarabotto[13], S. Schael[14], S. Scherl[54], M. Schiller[53],
H. Schindler[42], M. Schmelling[16], B. Schmidt[42], S. Schmitt[14], O. Schneider[43],
A. Schopper[42], M. Schubiger[32], S. Schulte[43], M.H. Schune[11], R. Schwemmer[42],
B. Sciascia[23,42], A. Sciuccati[42], S. Sellam[40], A. Semennikov[38], M. Senghi Soares[33],
A. Sergi[24,k], N. Serra[44], L. Sestini[28], A. Seuthe[15], Y. Shang[5], D.M. Shangase[77],
M. Shapkin[38], I. Shchemerov[38], L. Shchutska[43], T. Shears[54], L. Shekhtman[38],
Z. Shen[5], S. Sheng[4,6], V. Shevchenko[38], E.B. Shields[26,m], Y. Shimizu[11],
E. Shmanin[38], J.D. Shupperd[62], B.G. Siddi[21,i], R. Silva Coutinho[44], G. Simi[28],
S. Simone[19,f], M. Singla[63], N. Skidmore[56], R. Skuza[17], T. Skwarnicki[62],
M.W. Slater[47], I. Slazyk[21,i], J.C. Smallwood[57], J.G. Smeaton[49], E. Smith[44],
M. Smith[55], A. Snoch[32], L. Soares Lavra[9], M.D. Sokoloff[59], F.J.P. Soler[53],
A. Solomin[38,48], A. Solovev[38], I. Solovyev[38], F.L. Souza De Almeida[2],
B. Souza De Paula[2], B. Spaan[15,†], E. Spadaro Norella[25,l], E. Spiridenkov[38],
P. Spradlin[53], F. Stagni[42], M. Stahl[59], S. Stahl[42], S. Stanislaus[57],
O. Steinkamp[44], O. Stenyakin[38], H. Stevens[15], S. Stone[62,†], S. Stracka[29],
D. Strekalina[38], F. Suljik[57], J. Sun[27], L. Sun[67], Y. Sun[60], P. Svihra[56],
P.N. Swallow[47], K. Swientek[34], A. Szabelski[36], T. Szumlak[34], M. Szymanski[42],
S. Taneja[56], A.R. Tanner[48], M.D. Tat[57], A. Terentev[38], F. Teubert[42], E. Thomas[42],
D.J.D. Thompson[47], K.A. Thomson[54], H. Tilquin[55], V. Tisserand[9], S. T'Jampens[8],
M. Tobin[4], L. Tomassetti[21,i], X. Tong[5], D. Torres Machado[1], D.Y. Tou[3],
E. Trifonova[38], S.M. Trilov[48], C. Trippl[43], G. Tuci[6], A. Tully[43], N. Tuning[32,42],
A. Ukleja[36,42], D.J. Unverzagt[17], E. Ursov[38], A. Usachov[32], A. Ustyuzhanin[38],
U. Uwer[17], A. Vagner[38], V. Vagnoni[20], A. Valassi[42], G. Valenti[20],
N. Valls Canudas[75], M. van Beuzekom[32], M. Van Dijk[43], H. Van Hecke[61],
E. van Herwijnen[38], M. van Veghel[73], R. Vazquez Gomez[39], P. Vazquez Regueiro[40],
C. Vázquez Sierra[42], S. Vecchi[21], J.J. Velthuis[48], M. Veltri[22,v], A. Venkateswaran[62],
M. Veronesi[32], M. Vesterinen[50], D. Vieira[59], M. Vieites Diaz[43], H. Viemann[70],
X. Vilasis-Cardona[75], E. Vilella Figueras[54], A. Villa[20], P. Vincent[13], F.C. Volle[11],
D. vom Bruch[10], A. Vorobyev[38], V. Vorobyev[38], N. Voropaev[38], K. Vos[74], R. Waldi[17],
J. Walsh[29], C. Wang[17], J. Wang[5], J. Wang[4], J. Wang[3], J. Wang[67], M. Wang[5],
R. Wang[48], Y. Wang[7], Z. Wang[44], Z. Wang[3], Z. Wang[6], J.A. Ward[50,63],
N.K. Watson[47], D. Websdale[55], C. Weisser[58], B.D.C. Westhenry[48], D.J. White[56],
M. Whitehead[48], A.R. Wiederhold[50], D. Wiedner[15], G. Wilkinson[57],
M.K. Wilkinson[62], I. Williams[49], M. Williams[58], M.R.J. Williams[52], F.F. Wilson[51],
W. Wislicki[36], M. Witek[35], L. Witola[17], G. Wormser[11], S.A. Wotton[49], H. Wu[62],
K. Wyllie[42], Z. Xiang[6], D. Xiao[7], Y. Xie[7], A. Xu[5], J. Xu[6], L. Xu[3], M. Xu[50],
Q. Xu[6], Z. Xu[9], Z. Xu[6], D. Yang[3], S. Yang[6], Y. Yang[6], Z. Yang[5], Z. Yang[60],
Y. Yao[62], L.E. Yeomans[54], H. Yin[7], J. Yu[65], X. Yuan[62], E. Zaffaroni[43],
M. Zavertyaev[16], M. Zdybal[35], O. Zenaiev[42], M. Zeng[3], D. Zhang[7], L. Zhang[3],
S. Zhang[65], S. Zhang[5], Y. Zhang[5], Y. Zhang[57], A. Zharkova[38], A. Zhelezov[17],
Y. Zheng[6], T. Zhou[5], X. Zhou[6], Y. Zhou[6], V. Zhovkovska[11], X. Zhu[3], X. Zhu[7],
Z. Zhu[6], V. Zhukov[14,38], Q. Zou[4,6], S. Zucchelli[20,g], D. Zuliani[28], G. Zunica[56].

19

[1] Centro Brasileiro de Pesquisas Físicas (CBPF), Rio de Janeiro, Brazil
[2] Universidade Federal do Rio de Janeiro (UFRJ), Rio de Janeiro, Brazil
[3] Center for High Energy Physics, Tsinghua University, Beijing, China
[4] Institute Of High Energy Physics (IHEP), Beijing, China
[5] School of Physics State Key Laboratory of Nuclear Physics and Technology, Peking University, Beijing, China
[6] University of Chinese Academy of Sciences, Beijing, China
[7] Institute of Particle Physics, Central China Normal University, Wuhan, Hubei, China
[8] Université Savoie Mont Blanc, CNRS, IN2P3-LAPP, Annecy, France
[9] Université Clermont Auvergne, CNRS/IN2P3, LPC, Clermont-Ferrand, France
[10] Aix Marseille Univ, CNRS/IN2P3, CPPM, Marseille, France
[11] Université Paris-Saclay, CNRS/IN2P3, IJCLab, Orsay, France
[12] Laboratoire Leprince-Ringuet, CNRS/IN2P3, Ecole Polytechnique, Institut Polytechnique de Paris, Palaiseau, France
[13] LPNHE, Sorbonne Université, Paris Diderot Sorbonne Paris Cité, CNRS/IN2P3, Paris, France
[14] I. Physikalisches Institut, RWTH Aachen University, Aachen, Germany
[15] Fakultät Physik, Technische Universität Dortmund, Dortmund, Germany
[16] Max-Planck-Institut für Kernphysik (MPIK), Heidelberg, Germany
[17] Physikalisches Institut, Ruprecht-Karls-Universität Heidelberg, Heidelberg, Germany
[18] School of Physics, University College Dublin, Dublin, Ireland
[19] INFN Sezione di Bari, Bari, Italy
[20] INFN Sezione di Bologna, Bologna, Italy
[21] INFN Sezione di Ferrara, Ferrara, Italy
[22] INFN Sezione di Firenze, Firenze, Italy
[23] INFN Laboratori Nazionali di Frascati, Frascati, Italy
[24] INFN Sezione di Genova, Genova, Italy
[25] INFN Sezione di Milano, Milano, Italy
[26] INFN Sezione di Milano-Bicocca, Milano, Italy
[27] INFN Sezione di Cagliari, Monserrato, Italy
[28] Università degli Studi di Padova, Università e INFN, Padova, Padova, Italy
[29] INFN Sezione di Pisa, Pisa, Italy
[30] INFN Sezione di Roma La Sapienza, Roma, Italy
[31] INFN Sezione di Roma Tor Vergata, Roma, Italy
[32] Nikhef National Institute for Subatomic Physics, Amsterdam, Netherlands
[33] Nikhef National Institute for Subatomic Physics and VU University Amsterdam, Amsterdam, Netherlands
[34] AGH - University of Science and Technology, Faculty of Physics and Applied Computer Science, Kraków, Poland
[35] Henryk Niewodniczanski Institute of Nuclear Physics Polish Academy of Sciences, Kraków, Poland
[36] National Center for Nuclear Research (NCBJ), Warsaw, Poland
[37] Horia Hulubei National Institute of Physics and Nuclear Engineering, Bucharest-Magurele, Romania
[38] Affiliated with an institute covered by a cooperation agreement with CERN
[39] ICCUB, Universitat de Barcelona, Barcelona, Spain
[40] Instituto Galego de Física de Altas Enerxías (IGFAE), Universidade de Santiago de Compostela, Santiago de Compostela, Spain
[41] Instituto de Fisica Corpuscular, Centro Mixto Universidad de Valencia - CSIC, Valencia, Spain
[42] European Organization for Nuclear Research (CERN), Geneva, Switzerland
[43] Institute of Physics, Ecole Polytechnique Fédérale de Lausanne (EPFL), Lausanne, Switzerland
[44] Physik-Institut, Universität Zürich, Zürich, Switzerland
[45] NSC Kharkiv Institute of Physics and Technology (NSC KIPT), Kharkiv, Ukraine
[46] Institute for Nuclear Research of the National Academy of Sciences (KINR), Kyiv, Ukraine
[47] University of Birmingham, Birmingham, United Kingdom
[48] H.H. Wills Physics Laboratory, University of Bristol, Bristol, United Kingdom
[49] Cavendish Laboratory, University of Cambridge, Cambridge, United Kingdom
[50] Department of Physics, University of Warwick, Coventry, United Kingdom
[51] STFC Rutherford Appleton Laboratory, Didcot, United Kingdom

[52] School of Physics and Astronomy, University of Edinburgh, Edinburgh, United Kingdom

[53] School of Physics and Astronomy, University of Glasgow, Glasgow, United Kingdom

[54] Oliver Lodge Laboratory, University of Liverpool, Liverpool, United Kingdom

[55] Imperial College London, London, United Kingdom

[56] Department of Physics and Astronomy, University of Manchester, Manchester, United Kingdom

[57] Department of Physics, University of Oxford, Oxford, United Kingdom

[58] Massachusetts Institute of Technology, Cambridge, MA, United States

[59] University of Cincinnati, Cincinnati, OH, United States

[60] University of Maryland, College Park, MD, United States

[61] Los Alamos National Laboratory (LANL), Los Alamos, NM, United States

[62] Syracuse University, Syracuse, NY, United States

[63] School of Physics and Astronomy, Monash University, Melbourne, Australia, associated to [50]

[64] Pontifícia Universidade Católica do Rio de Janeiro (PUC-Rio), Rio de Janeiro, Brazil, associated to [2]

[65] Physics and Micro Electronic College, Hunan University, Changsha City, China, associated to [7]

[66] Guangdong Provincial Key Laboratory of Nuclear Science, Guangdong-Hong Kong Joint Laboratory of Quantum Matter, Institute of Quantum Matter, South China Normal University, Guangzhou, China, associated to [3]

[67] School of Physics and Technology, Wuhan University, Wuhan, China, associated to [3]

[68] Departamento de Fisica , Universidad Nacional de Colombia, Bogota, Colombia, associated to [13]

[69] Universität Bonn - Helmholtz-Institut für Strahlen und Kernphysik, Bonn, Germany, associated to [17]

[70] Institut für Physik, Universität Rostock, Rostock, Germany, associated to [17]

[71] Eotvos Lorand University, Budapest, Hungary, associated to [42]

[72] INFN Sezione di Perugia, Perugia, Italy, associated to [21]

[73] Van Swinderen Institute, University of Groningen, Groningen, Netherlands, associated to [32]

[74] Universiteit Maastricht, Maastricht, Netherlands, associated to [32]

[75] DS4DS, La Salle, Universitat Ramon Llull, Barcelona, Spain, associated to [39]

[76] Department of Physics and Astronomy, Uppsala University, Uppsala, Sweden, associated to [53]

[77] University of Michigan, Ann Arbor, MI, United States, associated to [62]

[a] Universidade Federal do Triângulo Mineiro (UFTM), Uberaba-MG, Brazil

[b] Central South U., Changsha, China

[c] Hangzhou Institute for Advanced Study, UCAS, Hangzhou, China

[d] Excellence Cluster ORIGINS, Munich, Germany

[e] Universidad Nacional Autònoma de Honduras, Tegucigalpa, Honduras

[f] Università di Bari, Bari, Italy

[g] Università di Bologna, Bologna, Italy

[h] Università di Cagliari, Cagliari, Italy

[i] Università di Ferrara, Ferrara, Italy

[j] Università di Firenze, Firenze, Italy

[k] Università di Genova, Genova, Italy

[l] Università degli Studi di Milano, Milano, Italy

[m] Università di Milano Bicocca, Milano, Italy

[n] Università di Modena e Reggio Emilia, Modena, Italy

[o] Università di Padova, Padova, Italy

[p] Università di Perugia, Perugia, Italy

[q] Scuola Normale Superiore, Pisa, Italy

[r] Università di Pisa, Pisa, Italy

[s] Università della Basilicata, Potenza, Italy

[t] Università di Roma Tor Vergata, Roma, Italy

[u] Università di Siena, Siena, Italy

[v] Università di Urbino, Urbino, Italy

[w] MSU - Iligan Institute of Technology (MSU-IIT), Iligan, Philippines

[†] Deceased